

A numerical study of tropical cross-tropopause transport by convective overshoots

J.-P. Chaboureau¹, J.-P. Cammas¹, J. Duron¹, P. J. Mascart¹, N. M. Sitnikov², and H.-J. Voessing³

¹Laboratoire d'Aérodynamique, Université Paul Sabatier and CNRS, Toulouse, France

²Central Aerological Observatory, Dolgoprudny, Russia

³Institute for Atmospheric Physics, University of Mainz, Germany

Received: 20 November 2006 – Published in Atmos. Chem. Phys. Discuss.: 12 December 2006

Revised: 16 March 2007 – Accepted: 30 March 2007 – Published: 10 April 2007

Abstract. Observations obtained during the Tropical Convection, Cirrus and Nitrogen Oxides (TROCCINOX) golden day have revealed the presence of ice particles up to 410 K (18.2 km) 2 km above the local tropopause. The case was investigated using a three-dimensional quadruply nested non-hydrostatic simulation and Meteosat Second Generation (MSG) observations. The simulation reproduced the measurements along the flight track fairly well. A reasonable agreement with MSG observations was also achieved: the 10.8- μm brightness temperature (BT) minimum of 187 K was reproduced (a value 6 K colder than the environmental cold-point temperature) as was the positive BT difference between the 6.2- and 10.8- μm bands, an overshoot signature. The simulation produced several overshooting plumes up to 410 K yielding an upward transport of water vapour of a few tons per second across the tropical tropopause. The estimated mass flux agrees with those derived from over tracer budgets, indicating that convection transports mass across the tropopause.

1 Introduction

Water vapour transport across the Tropical Tropopause Layer (TTL) is a key process for interpreting the observed increase in stratospheric water vapour of about 1% per year (Oltmans et al., 2000; Rosenlof et al., 2001), which influences the ozone layer and climate change. Half the increase in stratospheric water vapour is attributed to changes in methane and its oxidation (Etheridge et al., 1998) while the other half is believed to be due to water vapour transport across the tropical tropopause. The concentration of the water vapour transported in the stratosphere is controlled by the cold point, the coldest temperature. The air is eventually dehydrated by wa-

ter vapour condensing into ice, which then precipitates further. Various dehydration hypotheses have been proposed, including fast ascent in cumulus clouds (e.g., Danielsen, 1982, 1991), slow, large-scale ascent (e.g., Folkins et al., 1999), and convective overshoot followed by a radiative ascent (e.g., Sherwood and Dessler, 2000).

The Tropical Convection, Cirrus and Nitrogen Oxides-2 (TROCCINOX-2) campaign took place in the state of São Paulo, Brazil in early 2005. Three instrumented research aircrafts were operated to investigate the impact of tropical deep convection on the chemical composition of the troposphere and the lower stratosphere. During the golden day, on 4 February 2005, the mission of the Geophysica stratospheric aircraft was thunderstorm interception. Ice particles were observed up to an altitude of 410 K potential temperature, i.e. about 2 km above the local tropopause. Several items of observational evidence suggest that the particles originated from overshooting plumes that occurred during this severe convective event.

Here, this tropical convective event over land is investigated using a Cloud Resolving Model (CRM). Since a CRM resolves convective circulations, it is able to represent the overshoots with their cloud plumes that are missed by the global models. There are a few three-dimensional (3-D) numerical studies on convective overshoots across the tropopause using CRMs. Most of them consider an idealized framework showing cross-tropopause transport via mid-latitude deep convection (e.g. Skamarock et al., 2000; Wang, 2003; Mullendore et al., 2005). Other studies address the impact of convection in the TTL. Some cases do not produce overshoot penetrating above the cold point (Potter and Holton, 1995; Küpper et al., 2004) while others find deep overshoots that produce diabatic cooling near the tropopause (Kuang and Bretherton, 2004; Robinson and Sherwood, 2006).

Another novel aspect of the present work is the use of a 3-D quadruply nested numerical simulation initialised with

Correspondence to: J.-P. Chaboureau
(jean-pierre.chaboureau@aero.obs-mip.fr)

Table 1. Characteristics of the nested domains.

| Model number | Grid mesh (km) | Grid points (Nx Ny Nz) | Model start (UTC) |
|--------------|----------------|------------------------|-------------------|
| 1 | 30 | 75 75 90 | 00 |
| 2 | 10 | 160 160 90 | 00 |
| 3 | 2 | 360 256 90 | 00 |
| 4 | 0.625 | 400 400 90 | 18 |

operational weather forecast analyses. The framework of real meteorological conditions allows a direct comparison with the observations taken by the Geophysica along its flight track. In addition, the simulation was evaluated at the mesoscale against Meteosat Second Generation (MSG) observations. We adopted a model-to-satellite approach (Morcrette, 1991), in which satellite brightness temperature (BT) images were directly compared to BTs computed from predicted model fields. This approach is especially powerful in identifying discrepancies of cloud cover forecasts with BTs at 10.8- μm (Chaboureau et al., 2000, 2002). The model-to-satellite approach associated with the BT difference (BTD) technique can also verify specific forecasts such as cirrus cover (Chaboureau and Pinty, 2006) and dust occurrence (Chaboureau et al., 2007). The BTD technique is based on the contrasted absorption property of emitters (gas or particles) at two wavelengths. Positive BTDs between the 6.2- and 10.8- μm bands were used to identify convective overshoots (Schmetz et al., 1997). As the simulation was sufficiently realistic in reproducing some overshooting plumes, it was used to estimate water vapour and mass fluxes across the tropopause. The paper is organised as follows. Section 2 describes the model and the experimental design. Section 3 gives an overview of both the observation and the simulation of the convective event. Section 4 describes the overshooting plumes reaching the lower stratosphere. Section 5 presents the estimates of mass and water vapour transport in the lower stratosphere. Section 6 concludes the paper.

2 Model and experimental design

The numerical simulation was performed with the anelastic non-hydrostatic mesoscale model Meso-NH (Lafore et al., 1998). The two-way interactive grid-nesting method (Stein et al., 2000) enabled the simultaneous running of several models on the same vertical levels but with different horizontal resolutions. The lateral boundary conditions were given by large-scale operational analyses from the European Centre for Medium-Range Weather Forecasts (ECMWF) for the outermost model, and they were provided at every time step by the outer models for the inner models.

The case was simulated with quadruply nested models, with a horizontal grid spacing of 40, 10, 2.5 km and 625 m.

The vertical grid had 90 levels up to 27 km with a level spacing of 40 m close to the surface to 400 m at high altitude (including the TTL). A sponge layer was installed from 22 to 27 km in order to damp the upward-propagating gravity waves generated by convection. The different model grids covered a domain centred over São Paulo state in Brazil (see Table 1 for the various characteristics). The simulation was initialized at 00:00 UTC 4th February 2005. It was integrated forward for 18 h using the three outer models and keeping outputs every hour. At 18:00 UTC, i.e. 15:00 local time (LT, UTC minus 3 h), the approximate time of the Geophysica take-off, the simulation was integrated forward for 6 h using the four models and keeping outputs every ten minutes. The choice of the model configuration was a trade-off between high resolution and computing cost.

For the two coarser-resolution grids (40 and 10 km), the subgrid-scale convection was parametrized by a mass-flux convection scheme (Bechtold et al., 2001). For the inner grids (2.5 km and 625 m), the convection was explicitly resolved and the convection scheme was switched off. The microphysical scheme included the three water phases with five species of precipitating and non-precipitating liquid and solid water (Pinty and Jabouille, 1998), and a modified ice to snow autoconversion parameterization following Chaboureau and Pinty (2006). The turbulence parameterization was based on a 1.5-order closure (Cuxart et al., 2000). For the three outer models, the turbulent flux computations were purely vertical using the mixing length of Bougeault and Lacarrère (1989) while, for the inner model, they were fully three-dimensional based on the parameterization of Deardorff (1974). The radiative scheme was the one used at ECMWF (Gregory et al., 2000) including the Rapid Radiative Transfer Model (RRTM) parameterization (Mlawer et al., 1997). Synthetic BTs corresponding to the MSG observations were computed offline using the Radiative Transfer for Tiros Operational Vertical Sounder (RTTOV) code version 8.7 (Saunders et al., 2005).

3 Overview of the convective event

The time evolution of the convective event was first illustrated by the BT minimum at 10.8- μm in the model-3 domain (Fig. 1). The observed BT minimum had a diurnal evolution with a maximum of 250 K at 09:00 LT and values less than 220 K before 06:00 LT and after 12:00 LT. At 11:00 LT, the minimum BT dropped 35 K in one hour, which is characteristic of the triggering of deep convection. The time evolution was typical of convection over land with a regime of deep convection in the afternoon (e.g. Chaboureau et al., 2004; Guichard et al., 2004). A massive amount of convective available potential energy (CAPE) was present with maximum values larger than 3800 J kg⁻¹ at 13:00 LT. Once deep convection had been triggered, the coldest clouds occurred between 15:00 and 18:00 LT (during the

Geophysica flight). The diurnal evolution was rather well reproduced by the simulation. A minimum of 187 K (-86°C) was observed between 15:00 and 19:00 LT while the simulation gave 186 K at 16:00 LT. The close time-evolution of the convective events between the simulation and the MSG observation was confirmed at each hour (e.g. see Fig. 3). Note that this case occurred in a period with little organized convection over São Paulo state and it was well forecast in real time during the TROCCINOX campaign by the Mesoscale model operating in regional mode with a horizontal grid mesh of 30 km (Chaboureaud and Pinty, 2006).

The realism of the simulation was further illustrated by measurements obtained with the Fluorescent Advanced Hygrometer (FLASH), the Rosemount temperature sensor, and the Forward Scattering Spectrometer Probe (FSSP)-100 on board the Geophysica. The FLASH instrument (Sitnikov et al., 2007) is a water vapour sensor based on the Lyman- α fluorescence technique with an average time of 1 s and an accuracy of $0.2\ \mu\text{mol mol}^{-1}$ (or ppmv). The FSSP-100 is a laser-particle spectrometer that samples the size distribution of aerosols in four size ranges between 2.7 and $30\ \mu\text{m}$ (in that special case) every 2 s with an accuracy of 60% for the volume concentration. The observed and simulated relative humidity with respect to ice, and the total particle concentration recorded along the Geophysica flight are shown in Fig. 2. The altitude and the potential temperature are also shown.

On the first ascent, the Geophysica reached an altitude of 18.7 km allowing us to characterize the TTL. Following the climatology study of Gettelman and Forster (2002), the TTL can be locally defined as extending from the level of the lapse rate minimum at 10–12 km to the cold-point tropopause (CPT) at 16–17 km. When applied to the Geophysica observations, these criteria put the TTL base around 12 km and its top at 17.2 km with a CPT of -82.8°C and a potential temperature of 378 K. However, at 16.3 km both temperature and water vapour underwent a strong change in their vertical gradient, remaining almost constant over a 1.5-km layer, with local minima of -80.0°C and 3 ppmv, respectively. Therefore the 16.3 km altitude (or 362-K potential temperature) was taken to define the TTL top while the value of -80.0°C was taken as the environmental CPT.

Two ascents within the lower stratosphere were decided on by the pilot in order to fly over huge clouds. They are indicated by the vertical dashed lines, around 15:30 LT and 17:30 LT. During these two ascents, ice particles were detected by the FSSP-100 up to an altitude of 410 K, i.e. about 2 km above the local tropopause. The decrease of relative humidity detected by the FLASH hygrometer from 60% to 20% during the first ascent was correctly reproduced by the simulation. But at 17:30 LT the 40% relative humidity simulated was much lower than the 60% observed. The fact that the particles were found in subsaturated air suggested they originated from overshooting air parcels that mixed with stratospheric dry air.

Between the two ascents, the Geophysica flew over a dis-

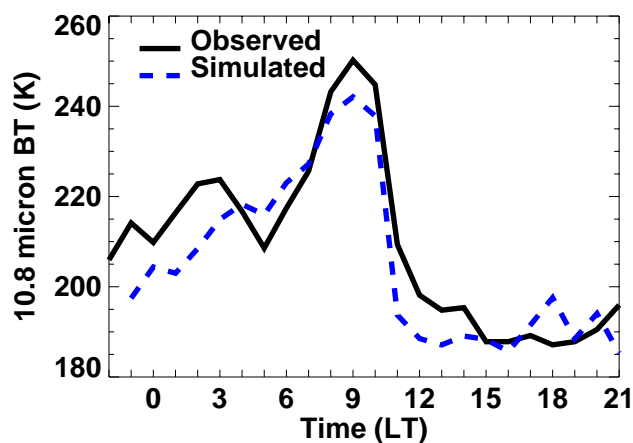


Fig. 1. Time evolution of observed and simulated minimum BT (K) at $10.8\ \mu\text{m}$ in the model-3 domain. The temporal resolution is 1 h.

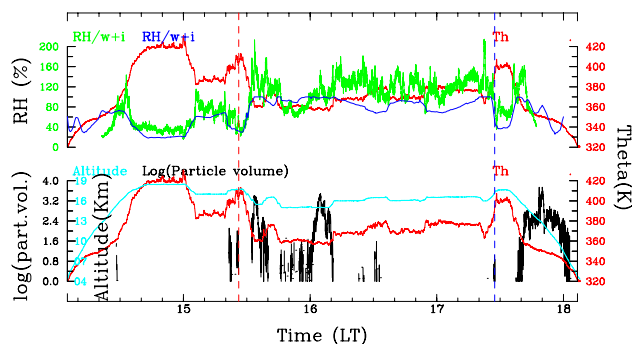


Fig. 2. Top: observed potential temperature (red line, K), relative humidity (green line, %) and simulated relative humidity (blue line, %) obtained during the Geophysica flight. Bottom: observed potential temperature (red line, K), altitude (cyan line, km), and total particle volume concentration (black line, $\mu\text{m}^3\ \text{cm}^{-3}$) as measured by the FSSP-100 instrument.

tance of 1500 km between 360 and 378 K, i.e. the TTL top and the CPT level. Supersaturation with respect to ice of up to 200% was observed with occasional presence of ice. In the simulation, saturation was sometimes achieved, but without any supersaturation as the bulk microphysics parameterization imposed a humidity adjustment to saturation. Furthermore, saturation was less frequently simulated than observed. This might be explained by expected differences in locations of the convective ascents between observation and simulation. In conclusion, the direct comparison with the Geophysica observations provided a fair qualitative agreement.

The convective event was then investigated at mesoscale by using satellite observations. Here the results are shown over the model-3 domain whose grid spacing ($2.5\ \text{km}$) corresponds to the MSG resolution (about $3.5\ \text{km}$ over the São

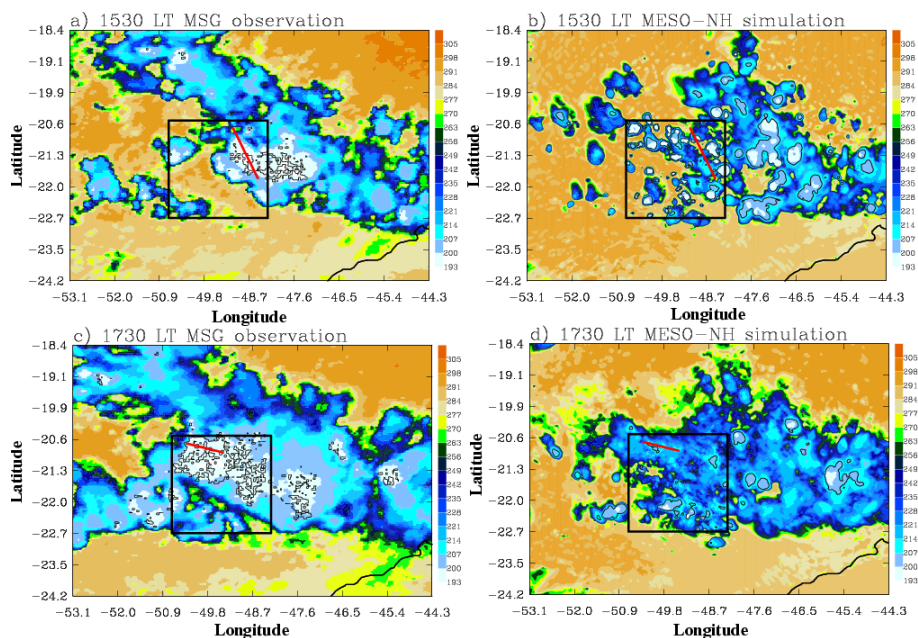


Fig. 3. (Left) Observed and (right) simulated MSG BTs over the model-3 domain at (top) 15:30 LT and (bottom) 17:30 LT on 4 February 2005. The colour scale indicates BT at $10.8\ \mu\text{m}$. The 3-K isoline of the BTD between 6.2- and $10.8\ \mu\text{m}$ band is superimposed. The red lines in the top and bottom panels indicate the Geophysica flight track between 15:15 and 15:30 LT, and 17:15 and 17:30 LT, respectively. The square shows the location of the model 4 domain.

Paulo state). Observed and simulated MSG BT at $10.8\ \mu\text{m}$ are shown for 15:30 and 17:30 LT, when ice particles were detected above 390 K (Fig. 3). The cloud systems sampled by the Geophysica were characterized by $10.8\ \mu\text{m}$ BTs of less than 193 K ($-80\ ^\circ\text{C}$), the coldest clouds being the thickest and deepest. The main cloud system was organized along a line that evolved from northwest-southeast to a zonal direction in two hours. In addition, convective overshoots were identified using satellite imagery with BTDs between the 6.2- and $10.8\ \mu\text{m}$ larger than 3 K. Overshoots were defined here as clouds with their tops located higher than the cold point altitude. In that case, BTs larger at $6.2\ \mu\text{m}$ than at $10.8\ \mu\text{m}$ can be explained by stratospheric water vapour, which absorbs radiation from the cold cloud top and emits radiation at higher stratospheric temperatures (Schmetz et al., 1997). The 3-K threshold was arbitrarily chosen to highlight the BTD signature. It is less than the empirical value of 5 K used by Roca et al. (2002) to analyse deep convection over the Indian Ocean. During the two Geophysica flight legs, BTDs over this particular threshold were effectively found over the coldest clouds, where particles were observed in the lower stratosphere.

The simulated low BTs at $10.8\ \mu\text{m}$ presented a line pattern similar to the observed ones (Fig. 3). However, there was not an exact match between the observed and the simulated individual cells, as can also be seen from the comparison along the flight track. For example, the westernmost cloud systems were missing. This might be ascribed to the absence of

smaller mesoscale features in the initial conditions and surface forcing. In the central part of the domain, the simulated convective cells appeared to be more scattered at 15:30 LT than the observed ones, resulting in a cluster at 17:30 LT with a larger BT minimum. This suggests a poor representation of the turbulent mixing between the in-cloud air and its environment. This is to be expected from a simulation with a 625-m horizontal grid spacing partly resolving turbulent fluxes of water vapour (e.g. Petch et al., 2002; Bryan et al., 2003; Petch, 2006). Finally, convective overshoots (as seen by BTDs larger than 3 K) were also simulated over the coldest clouds of several individual cells within and outside the model-4 domain (Fig. 3). In summary, the simulation reproduced the convective event reasonably well.

4 Overshooting plumes

The simulated overshooting plumes will now be investigated in the inner model (with a 625-m horizontal grid spacing). At 15:30 LT many cells reached the tropopause as seen with $10.8\ \mu\text{m}$ BT less than 193 K (Fig. 4). The coldest cloud tops were characterized with both a water vapour mixing ratio at 390 K larger than the background values of 4 ppmv (black isoline) and BTDs between the 6.2- and $10.8\ \mu\text{m}$ larger than 3 K (red isoline). The two fields do not exactly match as the former is a water vapour amount at a certain level while the latter is sensitive to the relative humidity (temperature and water vapour) integrated over the atmospheric column above

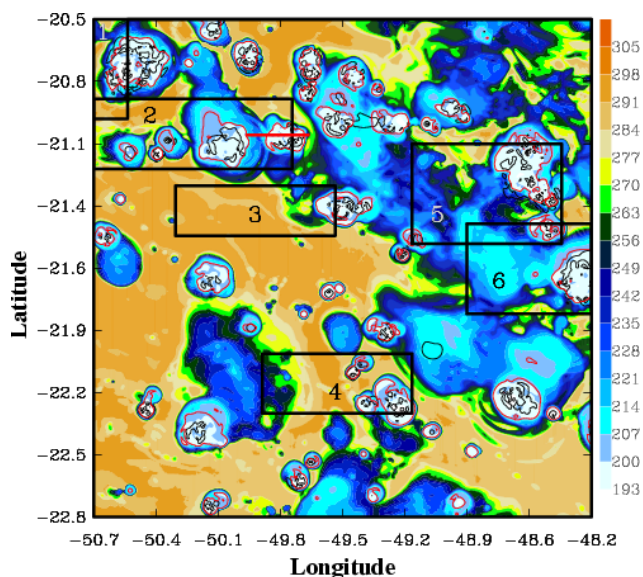


Fig. 4. High-resolution simulated fields in the model 4 domain at 15:30 LT: BT at $10.8\mu\text{m}$ (colour, K), BTD between 6.2- and $10.8\mu\text{m}$ band (3-K isoline in red), and water vapour mixing ratio over a 390-K potential temperature surface (4-ppmv isoline in black). The boxes indicate different sub-domains with occurrence of overshoots. The red line gives the position of the vertical cross-sections in Fig. 6.

the cloud top. This suggests that the BTD signal is an interesting indicator of water vapour anomalies in the stratosphere above the cloud tops reaching the cold point. Future work is needed to investigate the relationship between the BTD magnitude and the stratospheric water vapour anomalies. Such a radiative measure from space would further characterize the water vapour transport across the tropopause.

The time evolution of the maximum vertical velocities inside the inner model will now be examined (Fig. 5). A maximum of 76 m s^{-1} was reached at 15:20 LT. Such dramatic values have been reported for mid-latitude deep convective events with different CAPE amounts. Maximum vertical velocities of $50\text{--}55\text{ m s}^{-1}$ (60 m s^{-1}) have been observed (simulated) for a 3-D deep supercell storm characterized with an environment of 3012 J kg^{-1} CAPE (Wang, 2003). Mulendore et al. (2005) obtained a maximum of 88 m s^{-1} with a 1-km horizontal grid spacing 3-D simulation initialized with a sounding of very high CAPE (5034 J kg^{-1}). The latter gave a fairly good reproduction of a deep convective event with overshooting cloud tops reaching 18–19 km over Kansas where the tropopause height was at 13.5 km. Under tropical conditions, Robinson and Sherwood (2006) ran a series of 2-D simulations with increasing initial heating sources. As expected, the larger the CAPE, the higher the vertical velocity. Their simulation with a maximum CAPE of 3520 J kg^{-1} is characterized by a maximum of 55 m s^{-1} . After 15:20 LT the maximum vertical velocities decrease

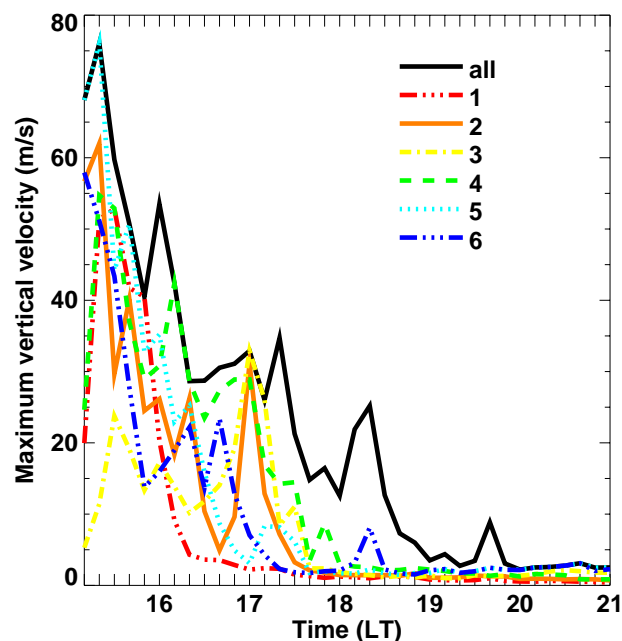


Fig. 5. Time evolution of the vertical velocity maximum (m s^{-1}). The results are given from the inner model for the whole domain and 6 boxes shown in Fig. 4. The temporal resolution is 10 min.

unevenly with time. The several secondary maximum up-draughts that occur every 60–80 min are the signature of separate cells growing and dissipating as shown by the maximum values for the different boxes (whose frames are displayed in Fig. 4). In box 5, the absolute maximum value of 76 m s^{-1} appears to be due to the interaction between two cells (not shown). Also at 15:20 LT a second maximum value of 62 m s^{-1} is obtained in box 2, but due to a single cell.

The convective event associated with the individual plume in box 2 is shown in detail with a series of vertical cross sections along the mean stratospheric flow (Fig. 6). At 15:10 LT an updraught from 3 to 18 km was already established, resulting in a plume of total water larger than 2 g kg^{-1} standing up to 15 km, a cloud top just below 370 K, and an out-flow at 14 km (as depicted by the $10^{-3}\text{ kg kg}^{-1}$ red line). The diabatic heating within the updraught resulted in a 4-km lowering of the 350-K isentrope. The environment, already perturbed by previous convective activities, was characterized by a vertical decrease of the total water, with two remarkable values, 5 g kg^{-1} near the freezing level (around 4–5 km) and 0.25 g kg^{-1} (around 4 ppmv) at 370 K. (This 4 ppmv background value came from the ECMWF analysis and is slightly larger than the 3 ppmv measured during the first Geophysica ascent.) At 15:20 LT the updraught attained its climax with the vertical plume and its associated cloud cover reaching 19 km. The layer between 350 and 370 K had doubled in thickness. At 17 km the rising air was first adiabatically cooled, resulting in a mean decrease of the CPT to

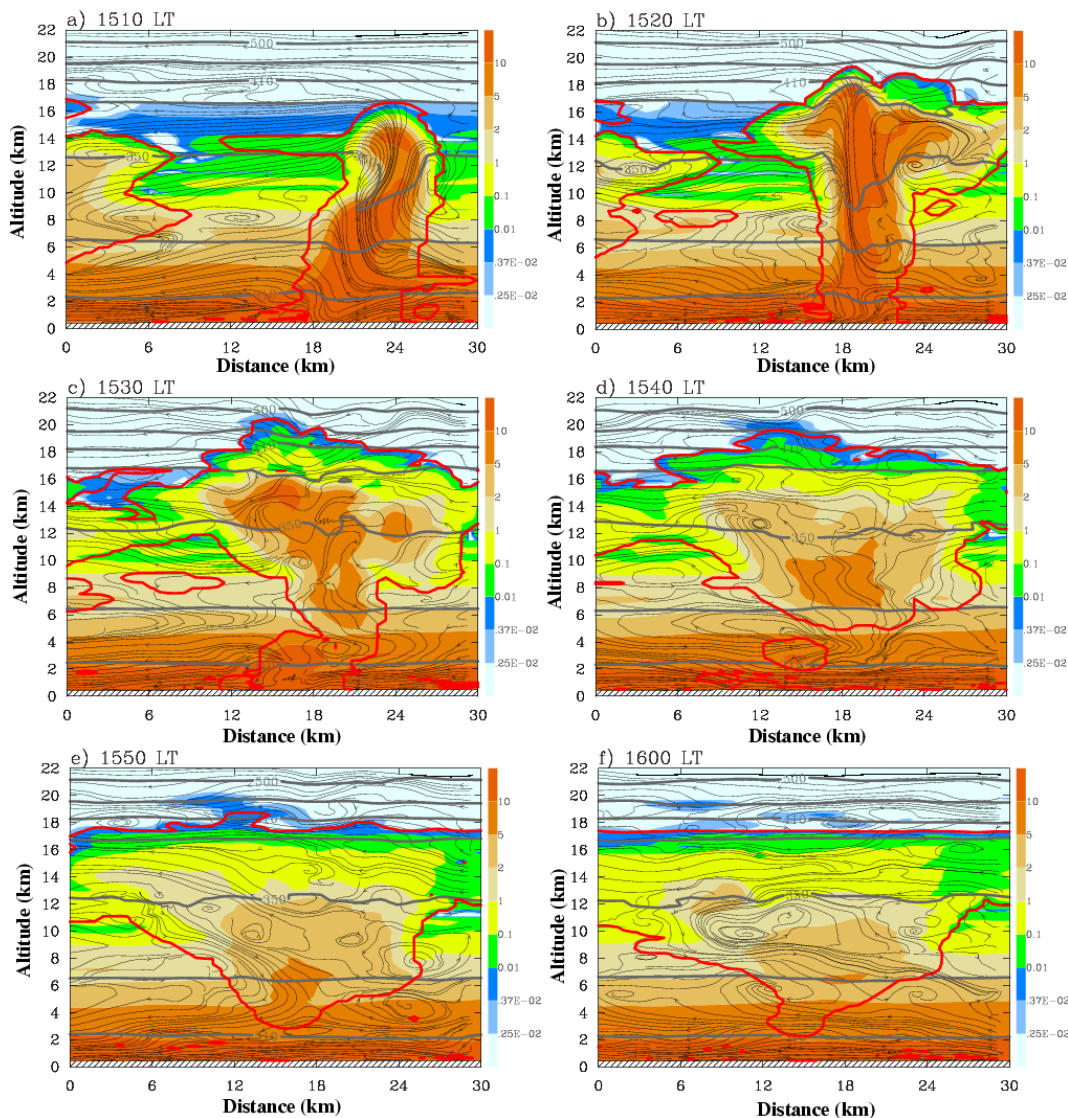


Fig. 6. Vertical cross section of the total water mixing ratio (g kg^{-1}) at 15:10, 15:20, 15:30, 15:40, 15:50, and 16:00 LT 4 February 2005 along the line shown in Fig. 4. Black lines are the stream functions along the cross-section. Grey contours represent potential temperatures (intervals 310, 330, 350, 370, 410, 450, and 500 K). The red line delineates the cloud limit with condensed water mixing ratio larger than $10^{-3} \text{ kg kg}^{-1}$. The vertical axis range is 0–22 km and horizontal axis range 0–30 km. The aspect ratio is 1.

-88°C . The saturation mixing ratio was sufficiently reduced so that it could locally yield to air dehydration where ice sedimentation was fast enough. But the vertical motion was so strong that ascending air crossed isentropes in the lower stratosphere.

At 15:30 LT the updraught ended leaving a perturbed circulation. In the troposphere below 15 km, many rotors mix environmental air with the cloud. In the lower stratosphere the cloud top drifted 6 km westward with water vapour larger 4 ppmv found up to 20 km. At 18:40 and 15:50 LT the atmosphere continued to recover from the convective burst and the cloud dissipated by precipitation and mixing. In the lower stratosphere, water vapour anomalies over 0.37 g kg^{-1}

(around 6 ppmv) remained. Finally at 16:00 LT the cloud top was at 17 km all along the cross section. Within the troposphere, the dissipation of cloud by hydrometeor precipitation continued. Above the cloud cover, between 17 and 20 km, the pockets of water vapour anomalies stretched into thin layers with a mixing ratio larger than 6 ppmv. This clearly shows that an individual overshooting plume can transport and deposit moisture into the stratosphere.

Figure 7 shows the temperature profile at 15:10 and 15:20 LT where the stratospheric penetration occurs (from 18 km to the y-axis in Fig. 6). At 15:10 LT, the simulated temperature profile is representative of environmental conditions with an adiabatic gradient of $-10^\circ\text{C km}^{-1}$ up to

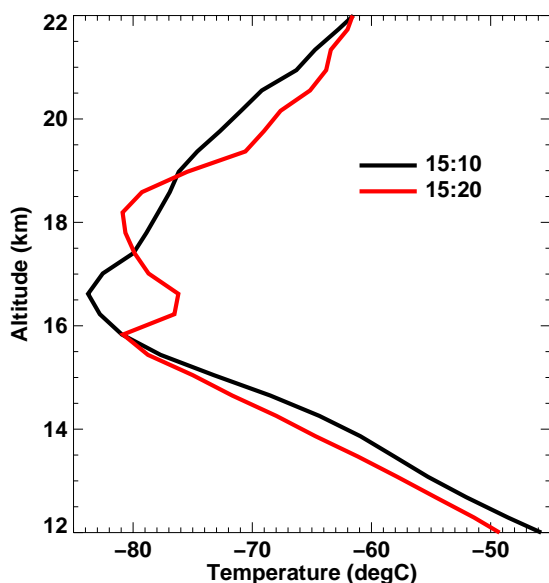


Fig. 7. Vertical profiles of temperature at (black) 15:10 and (red) 15:20 LT where stratospheric penetration occurs from 18 km to the y-axis in Fig. 6.

16.6 km and a temperature increase aloft. At 15:20 LT, the temperature in the lower stratosphere is perturbed with lower (higher) temperatures at 18 km (16.6 km) than at 15:10 LT. The resulting temperature profile presents two minima, one 1 km lower than the environment CTP, the other 2 km higher in the stratosphere. The change in temperature fully corroborates the hypothesis of Danielsen (1982).

5 Mass and water vapour transport

The impact of such a deep convective event on the composition of the stratosphere will now be discussed. The cross-isentropic water vapour transport is given over the model-3 domain. The transport of water vapour was calculated by summing the values of positive vertical flux across isentropic surface for different values of potential temperature. As expected, the resulting water vapour fluxes were the largest at 16:00 LT and these maximum values decreased with increasing potential temperature (Fig. 8). It is worth noting that the peak value of 8 tons s^{-1} obtained across the 380-K surface matches the value simulated by Wang (2003) for a North-American Midwest severe thunderstorm.

A further estimate of the total mass flux is shown in Fig. 9 following the presentation of Küpper et al. (2004). The mass flux derived from the simulation was obtained after averaging over the model-3 domain and over the 24 h of the simulation. The results derived from previous studies are also shown. All the mass flux estimates show decreasing values with altitude but for different ranges within the TTL. The present CRM results form an upper bound to those derived from

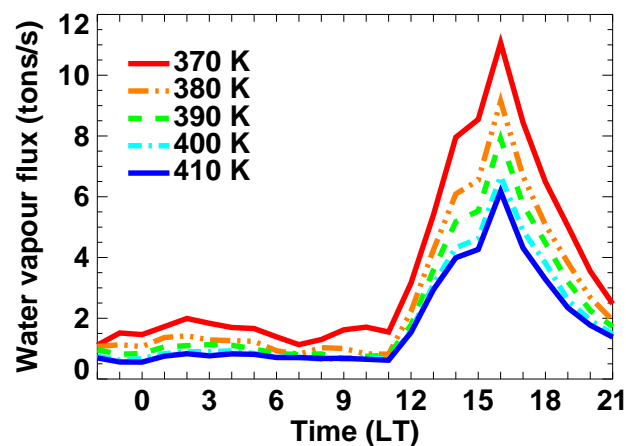


Fig. 8. Time series of upward water vapour flux through isentropic surface of 370, 380, 390, 400, and 410 K over the model-3 domain. The temporal resolution is 1 h.

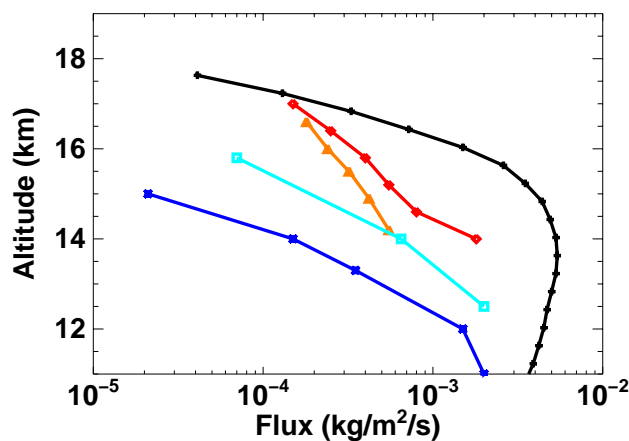


Fig. 9. Mass flux estimates based on O_3 (red diamonds) and CO (orange triangles) budgets (Dessler, 2002), cloud imagery (cyan squares; Gettelman et al., 2002), and cloud-resolving simulation from Küpper et al. (2004) (blue asterisks) and this work (black crosses).

O_3 and CO budgets by Dessler (2002) indicating that convection transports mass at the tropopause. These estimates are two orders of magnitude greater than the mass flux obtained by Küpper et al. (2004) from a CRM simulation (run to a radiative-convective equilibrium) representative of maritime conditions. The present estimate is also larger than the one obtained from cloud imagery and re-analysis temperatures by Gettelman et al. (2002). Based on BTs at $11 \mu\text{m}$ colder than the tropopause, they found that convection rarely penetrated more than 1.5 km above the tropopause.

However, recent studies on tropical overshoots have shown that these cases are not so infrequent. Liu and Zipser (2005) use a 5-year Tropical Rainfall Measuring Mission (TRMM) database to detect large lifted ice particles that overshoot.

Their overshooting criteria search for 20 km² pixels with more than 20 dBZ of radar reflectivity above a reference height. They find that 1.3% of tropical convection systems reach 14 km and 0.1% of them may even penetrate the 380-K potential temperature level. Furthermore, stronger overshooting has been found over land, including South America (Liu and Zipser, 2005). Another study from Geoscience Laser Altimeter System (GLAS) observations find more frequent occurrence of thick clouds in the TTL and above the tropopause than other studies, due to the high spatial resolution of the lidar, with 76.8 m in the vertical and 1.4 km in the horizontal. Dessler et al. (2006) found that 3.0% and 19% of the thick and thin cloud observations, respectively, showed a cloud top in the TTL and 0.34% and 3.1% showed a cloud top above the average level of the tropopause.

Finally, in the absence of vertical shear, the individual event studied here remained localized. A satellite analysis of convective systems over the Indian Ocean shows that, for mesoscale organized convection (spanning an area larger than 10⁴ km²), the larger the deepest systems, the larger the fraction of overshoot areas (Roca et al., 2002). It is anticipated that more import of water vapour in the stratosphere should be found over organized systems as was observed during the African Monsoon Multidisciplinary Analysis (AMMA) campaign (J.-P. Pommereau 2006, personal communication).

6 Conclusions

The paper presents a numerical study of the TROCCINOX golden day. For the first time in the framework of real meteorological conditions, a tentative estimate of mass fluxes across the TTL is given for a tropical case simulated by a CRM. Comparisons with observations show the good overall quality of the simulation. The convective event builds up in time with minimum BT at 10.8- μ m between 15:00 and 18:00 LT. In particular, the BT minimum of 187 K is reproduced, a value 6 K colder than the environmental cold-point temperature. At local scale, the moisture variation measured during the Geophysica flight is captured. At mesoscale, the thickest and deepest clouds are correctly organized in line with overshooting cells and positive BTD between the 6.2- and 10.8- μ m bands on the top. Moreover, a simulated overshoot supports the explanation for the presence of particles up to 410 K. Upward water vapour mass fluxes are of the same order of magnitude as those of a midlatitude case. Day-averaged mass fluxes derived from the simulation are also consistent with a global budget study. All these elements support the scenario of deep convective overshoots from troposphere-stratosphere exchange.

This numerical study suffers, however, from uncertainties that need to be alleviated. First, the framework of real meteorological conditions imposes the simulation with grid mesh of few hundred metres. This may result in a poor represen-

tation of the turbulent mixing between the in-cloud air and its environment within the troposphere, and the gravity wave breaking aloft. Therefore, a higher-resolution simulation will be run under an idealized framework. Then, the cloud microphysics used here cannot allow supersaturation to occur, in contradiction with the observations in the upper troposphere. This may result in an excess of latent heat release by condensation. The sensitivity to a more elaborate cloud scheme, like a double-moment scheme, will require further study. Finally the use of passive tracers would give a more quantitative cross-tropopause transport in such very intense deep convective events. The coming idealized case study will take advantage of measurements that have been not used here, such as trace gases, aerosol profiles, and lightning activity. The present case represents a single tropical convective event. A higher wind shear environment would enhance the cross-tropopause transport by a wave breaking more easily in the stratosphere. There is a strong need to study such cases (e.g. squall line and other tropical mesoscale convective systems). Another critical numerical issue concerns the fate of positive water vapour anomalies after the stratospheric penetration. This issue could be addressed with the combination of high-resolution runs and large-scale models only, which run for sufficiently long periods in the framework of super-parametrization or global (at least regional) CRM.

Acknowledgements. We are grateful to J.-P. Pinty and the three anonymous reviewers for their helpful comments. This research was supported by the TROCCINOX project funded by the European Commission under contract EVK2-CT-2001-00122. Computer resources were allocated by IDRIS. MSG observations were provided by SATMOS.

Edited by: R. MacKenzie

References

- Bechtold, P., Bazile, E., Guichard, F., Mascart, P., and Richard, E.: A mass flux convection scheme for regional and global models, *Quart. J. Roy. Meteorol. Soc.*, 127, 869–886, 2001.
- Bougeault, P. and Lacarrère, P.: Parameterization of orographic induced turbulence in a mesobetascale model, *Mon. Weather Rev.*, 117, 1872–1890, 1989.
- Bryan, G. H., Wyngaard, J. C., and Fritsch, J. M.: Resolution requirements for the simulation of deep moist convection, *Mon. Weather Rev.*, 131, 2394–2416, 2003.
- Chaboureau, J.-P. and Pinty, J.-P.: Evaluation of a cirrus parameterization with Meteosat Second Generation, *Geophys. Res. Lett.*, 33, L03815, doi:10.1029/2005GL024725, 2006.
- Chaboureau, J.-P., Cammas, J.-P., Mascart, P., Pinty, J.-P., Claud, C., Roca, R., and Morcrette, J.-J.: Evaluation of a cloud system life-cycle simulated by Meso-NH during FASTEX using METEOSAT radiances and TOVS-3I cloud retrievals, *Quart. J. Roy. Meteorol. Soc.*, 126, 1735–1750, 2000.
- Chaboureau, J.-P., Cammas, J.-P., Mascart, P., Pinty, J.-P., and Lafore, J.-P.: Mesoscale model cloud scheme assessment us-

- ing satellite observations, *J. Geophys. Res.*, 107(D17), 4301, doi:10.1029/2001JD000714, 2002.
- Chaboureaud, J.-P., Guichard, F., Redelsperger, J.-L., and Lafore, J.-P.: The role of stability and moisture in the development of convection, *Quart. J. Roy. Meteorol. Soc.*, 130, 3105–3117, 2004.
- Chaboureaud, J.-P., Tulet, P., and Mari, C.: Diurnal cycle of dust and cirrus over West Africa as seen from Meteosat Second Generation satellite and a regional forecast model, *Geophys. Res. Lett.*, 34, L02822, doi:10.1029/2006GL027771, 2007.
- Cuxart, J., Bougeault, P., and Redelsperger, J.-L.: A turbulence scheme allowing for mesoscale and large-eddy simulations, *Quart. J. Roy. Meteorol. Soc.*, 126, 1–30, 2000.
- Danielsen, E. F.: A dehydration mechanism for the stratosphere, *Geophys. Res. Lett.*, 9(6), 605–608, 1982.
- Danielsen, E. F.: In situ evidence of rapid, vertical, irreversible transport of lower tropospheric air into the lower tropical stratosphere by convective cloud turrets and by larger-scale upwelling in tropical cyclones, *J. Geophys. Res.*, 98(D5), 8665–8681, 1991.
- Deardorff, J. W.: Three-dimensional numerical study of turbulence in an entraining mixed layer, *Bound. Layer. Meteorol.*, 7, 199–216, 1974.
- Dessler, A. E.: The effect of deep, tropical convection on the tropical tropopause layer, *J. Geophys. Res.*, 107(D3), 4033, doi:10.1029/2001JD000511, 2002.
- Dessler, A. E., Palm, S. P., and Spinhirne, J. D.: Tropical cloud-top height distributions revealed by the Ice, Cloud, and Land Elevation Satellite (ICESat)/Geoscience Laser Altimeter System (GLAS), *J. Geophys. Res.*, 111, D12215, doi:10.1029/2005JD006705, 2006.
- Etheridge, D. M., Steele, L. P., Francey, R. J., and Langenfelds, R. L.: Atmospheric methane between 1000 A.D. and present: Evidence of anthropogenic emissions and climatic variability, *J. Geophys. Res.*, 103(D13), 15 979–15 994, 1998.
- Folkens, I., Loewenstein, M., Podolske, J., Oltmans, S. J., and Profitt, M.: A barrier to vertical mixing at 14 km in the tropics: Evidence from ozonesondes and aircraft measurements, *J. Geophys. Res.*, 104(D18), 22 095–22 102, 1999.
- Gottelman, A. and Forster, P. M. D. F.: Definition and climatology of the tropical tropopause layer, *J. Meteor. Soc. Japan*, 80, 911–924, 2002.
- Gottelman, A., Salby, M. L., and Sassi, F.: Distribution and influence of convection in the tropical tropopause region, *J. Geophys. Res.*, 107(D10), 408026, 1601–1604, 2002.
- Gregory, D., Morcrette, J.-J., Jakob, C., Beljaars, A. M., and Stockdale, T.: Revision of convection, radiation and cloud schemes in the ECMWF model, *Quart. J. Roy. Meteorol. Soc.*, 126, 1685–1710, 2000.
- Guichard, F., Petch, J. C., Redelsperger, J.-L., Bechtold, P., Chaboureaud, J.-P., Cheinet, S., Grenier, H., Grabowski, W., Jones, C. J., Köhler, M., Pirou, J.-M., Tailleux, R., and Tomasini, M.: Modelling the diurnal cycle of deep precipitating convection over land with cloud-resolving models and single-column models, *Quart. J. Roy. Meteorol. Soc.*, 130, 3139–3172, 2004.
- Kuang, Z. and Bretherton, C. S.: Convective influence on the heat balance of the tropical tropopause layer: a cloud-resolving model study, *J. Atmos. Sci.*, 61, 2919–2927, 2004.
- Küpper, C., Thuburn, J., Craig, G. C., and Birner, T.: Mass and water transport into the tropical stratosphere: A cloud-resolving simulation, *J. Geophys. Res.*, 109, D10111, doi:10.1029/2004JD004541, 2004.
- Lafore, J.-P., Stein, J., Asencio, N., Bougeault, P., Ducrocq, V., Duron, J., Fischer, C., Hérelil, P., Mascart, P., Masson, V., Pinty, J.-P., Redelsperger, J.-L., Richard, E., and Vilà-Guerau de Arellano, J.: The Meso–NH Atmospheric Simulation System. Part I: adiabatic formulation and control simulations. Scientific objectives and experimental design, *Ann. Geophys.*, 16, 90–109, 1998, <http://www.ann-geophys.net/16/90/1998/>.
- Liu, C. and Zipser, E. J.: Global distribution of convection penetrating the tropical tropopause, *J. Geophys. Res.*, 110, D23104, doi:10.1029/2005JD006063, 2005.
- Mlawer, E. J., Taubman, S. J., Brown, P. D., Iacono, M. J., and Clough, S. A.: Radiative transfer for inhomogeneous atmospheres: RRTM, a validated correlated-k model for the longwave, *J. Geophys. Res.*, 102D, 16 663–16 682, 1997.
- Morcrette, J.-J.: Evaluation of model-generated cloudiness: Satellite-observed and model-generated diurnal variability of brightness temperature, *Mon. Weather Rev.*, 119, 1205–1224, 1991.
- Mullendore, G. L., Durran, D. R., and Holton, J. R.: Cross-tropopause tracer transport in midlatitude convection, *J. Geophys. Res.*, 110, D06113, doi:10.1029/2004JD005059.536–549, 2005.
- Oltmans, S. J., Vömel, H., Hofmann, D. J., Rosenlof, K. H., and Kley, D.: The increase in stratospheric water vapor from balloonborne, frostpoint hygrometer measurements at Washington, D.C., and Boulder, *Geophys. Res. Lett.*, 27(21), 3453–3456, 2000.
- Petch, J.: Sensitivity studies of developing convection in cloud-resolving model, *Quart. J. Roy. Meteor. Soc.*, 132, 345–358, 2006.
- Petch, J. C., Brown, A. R., and Gray, M. E. B.: The impact of horizontal resolution on convective development in simulations of the diurnal cycle over land, *Quart. J. Roy. Meteorol. Soc.*, 128, 2031–2044, 2002.
- Pinty, J.-P. and Jabouille, P.: A mixed-phase cloud parameterization for use in a mesoscale non-hydrostatic model: simulations of a squall line and of orographic precipitations, in: Proc. AMS conference on cloud physics, 17–21 August 1998, Everett, Wa, USA, 217–220, 1998.
- Potter, B. E. and Holton, J. R.: The Role of Monsoon Convection in the Dehydration of the Lower Tropical Stratosphere, *J. Atmos. Sci.*, 52, 1034–1050, 1995.
- Robinson, F. J. and Sherwood, S. C.: Modeling the impact of convective entrainment on the tropical tropopause, *J. Atmos. Sci.*, 63, 1013–1027, 2006.
- Roca, R., Viollier, M., Picon, L., and Desbois, M.: A multi satellite analysis of deep convection and its moist environment over the Indian Ocean during the winter monsoon, *J. Geophys. Res.*, 107, 8012, doi:10.1029/2000JD000040, 2002.
- Rosenlof, K. H. I., Chiou, E.-W., Chu, W. P., Johnson, D. G., Kelly, K. K., Michelsen, H. A., Nedoluha, G. E., Remsburg, E. E., Toon, G. C., and McCormick, M. P.: Stratospheric water vapor increases over the past half-century, *Geophys. Res. Lett.*, 28(7), 1195–1198, 2001.
- Saunders, R., Matricardi, M., Brunel, P., English, S., Bauer, P., O’Keefe, U., Francis, P., and Rayer, P.: RTTOV-8 Science and

- validation report, Tech. rep., NWP SAF Report, 41 p., 2005.
- Schmetz, J., Tjemkes, S. A., Gube, M., and van de Berg, L.: Monitoring deep convection and convective overshooting with METEOSAT, *Adv. Space Res.*, pp. 433–441, 1997.
- Sherwood, S. C. and Dessler, A. E.: On the control of stratospheric humidity, *Geophys. Res. Lett.*, 58, 2513–2516, 2000.
- Sitnikov, N. M., Yushkov, V. A., Afchine, A. A., Korshunov, L. I., Astakhov, V. I., Ulanovskii, A. E., Kraemer, M., Mangold, A., Schiller, C. and Ravegnani, F.: The FLASH instrument for water vapor measurements on board the high-altitude airplane, *Prib. Tekh. Eksp.*, 50, 121129, 2007. [*Instrum. Exp. Tech. (Engl. Transl.)*, 50, 113–121, 2007].
- Skamarock, W. C., Powers, J. G., Barth, M., Dye, J. E., Matejka, T., Bartels, D., Baumann, K., Stith, J., Webster, C. R., Grecu, J., Loewenstein, M., Podolske, J. R., Parrish, D. D., and Hubler, G.: Numerical simulations of the 10 July Stratospheric-Tropospheric Experiment: Radiation, Aerosols, and Ozone/Deep Convection Experiment convective system: Kinematics and transport, *J. Geophys. Res.*, 105(D15), 19 973–19 990, 2000.
- Stein, J., Richard, E., Lafore, J.-P., Pinty, J.-P., Asencio, N., and Cosma, S.: High-resolution non-hydrostatic simulations of flash-flood episodes with grid-nesting and ice-phase parameterization, *Meteorol. Atmos. Phys.*, 72, 203–221, 2000.
- Wang, P. K.: Moisture plumes above thunderstorm anvils and their contributions to cross-tropopause transport of water vapor in midlatitudes, *J. Geophys. Res.*, 108(D6), 4194, doi:10.1029/2002JD002581, 2003.